ELSEVIER

www.elsevier.nl/locate/ica

Inorganica Chimica Acta 304 (2000) 137–143

Inorganica Chimica Acta

Note

Solution and solid study of Zn(II) and Cd(II) complexes with *N*-(6-amino-3,4-dihydro-3-methyl-5-nitroso-4-oxo-pyrimidin-2-yl)-glycine as ligand. Crystal structures of $[ZnL_2(H_2O)_4]\cdot 6H_2O$ and $\{[Cd(\mu\text{-}L)Cl(H_2O)_2]\cdot H_2O\}_n$

P. Arranz-Mascarós [a], R. López-Garzón* [a,1], M.D. Gutierrez-Valero [a],
M.L. Godino-Salido [a], J.M. Moreno* [b,2]

[a] *Departamento de Química Inorgánica y Orgánica, Facultad de Ciencias Experimentales, Universidad de Jaén, 23071-Jaén, Spain*
[b] *Departamento de Química Inorgánica, Facultad de Ciencias, Universidad de Granada, 18071-Granada, Spain*

Received 15 September 1999; accepted 21 January 2000

Abstract

Reactions of *N*-(4-amino-1,6-dihydro-1-methyl-5-nitroso-6-oxo-pyrimidin-2-yl)glycine with Zn(II) and Cd(II) (1:1 and 1:4 metal/ligand ratios, in aqueous media at 35°C and 0.1 M KCl ionic strength) were studied by potentiometric methods. This study has revealed a similar qualitative behaviour to that found by us for this family of *N*-pyrimidine aminoacids, the primary coordination site being either the pyrimidine or the carboxylate group depending on whether the ligand acts in neutral form or deprotonated, respectively. In solid state two complexes were obtained by working in 1:1 metal-to-ligand ratio: $[Zn(L)_2(H_2O)_4]\cdot 6H_2O$ and $\{[Cd(\mu\text{-}L)Cl(H_2O)_2]\cdot H_2O\}_n$, which were characterised by IR and NMR spectroscopies, TG and DSC techniques and single crystal X-ray diffraction. The former complex is mononuclear with the Zn(II) ion hexacoordinated in a distorted octahedral geometry. The coordination sphere is formed by four water molecules and two ligands coordinating in a monodentate fashion through the carboxylate group. The Cd(II) complex consists of a 1D infinite chain, with the metal ion heptacoordinated in a distorted pentagonal bipyramid. The ligand bridges the metal ions coordinating in a bis-didentate fashion through the pyrimidine and the carboxylate group. The nature of these complexes is very different to that shown by the Zn(II) and Cd(II) complexes with the related methionine derivative, which is attributed to he effect of the R substituent on the aminoacid moiety. © 2000 Elsevier Science S.A. All rights reserved.

Keywords: Crystal structures; Zinc complexes; Cadmium complexes; Amino acid complexes

1. Introduction

It is well known that both pyrimidine bases and α-aminoacids act as ligands toward metal ions. Actually, metal complexes of these ligands are of interest and have been extensively studied. In this line we are working with a new family of ligands containing both fragments (Scheme 1), by which could be described as *N*-substituted α-amino acids as well as pyrimidine derivatives. The synergic effect of both moieties makes of this kind of compounds a versatile ligands showing different coordination patterns, which can be tuned to give rise metal complexes ranging from mononuclear to 1D, 2D and 3D polynuclear. The coordination modes of *N*-substituted α-aminoacids depend on the nature of

---

[1] *Corresponding author. Tel.: + 39-9-5824 3322; fax: + 34-9-5824 8526.

[2] *Corresponding author. Tel.: + 39-9-5824 3322; fax: + 34-9-5824 8526; e-mail: jmoreno@ugr.es

PII: S0020-1693(00)00070-0

the substituent. Thus, *N*-alkyl derivatives enhance the basicity of the NH group [1–5], while electronic attractive substituents (such as pyrimidine bases) reduce the basicity of the amino group coordinating to the metal ion through the carboxylate group [6–9]. In addition to this, a certain number of factors govern the coordination behaviour of *N*-pyrimidine α-aminoacids ligands, among others, the R-group on the C_α (see Scheme 1), the nature of the metal ion and the pH. Our aqueous solution studies have show that in neutral or slightly basic medium these ligands coordinate through the deprotonated carboxylate group, while in acidic medium the carboxylate group remains protonated and interactions take place through the exocyclic oxo and nitroso groups belonging to the pyrimidine moiety (Scheme 1) [7–10].

In the present paper we study the reactivity of Zn(II) and Cd(II) ions with *N*-2-(4-amino-1,6-dihydro-1-methyl-5-nitroso-6-oxopyrimidinyl)glycine (HL), in aqueous solution and in solid state, and the results are compared to those obtained by us for related systems.

2. Experimental

The ligand was obtained by following a previously reported procedure [10]. Nanopure water was used as solvent for potentiometric measurements. Standardised KOH, HCl, $ZnCl_2$ and $CdCl_2$ aqueous solutions (Merck) were also used. All the potentiometric measurements were carried out in 0.1 M KCl as background electrolyte.

C, H and N microanalyses were performed with a Fison's EA-1109 instrument. IR and NMR spectra, and TG and DSC diagrams were obtained as already reported [8]. The potentiometric assembly was described in a previous work [11], and the pH measurements were carried out with a calomel K4040 and a glass G2040B Radiometer electrodes.

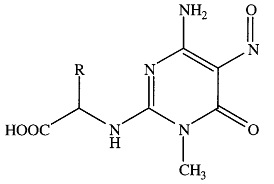

HL R=H
HL[1] $R=CH_2CH_2SCH_3$
HL[2] $R=CH_3$
HL[3] $R=CH(CH_3)_2$

Scheme 1.

2.1. Potentiometric measurements

Previously acidified aqueous solutions containing Zn(II)/HL mixtures ($[HL]=10^{-3}$ M) in 1:1 and 1:4 molar ratios, were titrated potentiometrically with 0.1 M KOH at 35°C and 0.1 M KCl ionic strength in order to study the complex formation processes. The pH range investigated was usually 2.5–7.5, before the $Zn(OH)_2$ precipitation.

Calibration of electrodes (Gran's method [12]) and the ionic product of the medium [13] was through the titration of known amounts of HCl with CO_2-free KOH solutions. The BEST program [14] was used to calculate the formation constants. In these calculations, previously reported values of protonation constants of the ligand were used [10]. The species formed in the equilibria are labelled by the pqr parameters, which define the number of metal ions, deprotonated ligands and protons, respectively.

2.2. Preparation of the complexes

2.2.1. $[Zn(L)_2(H_2O)_4]\cdot 6H_2O$ (**1**)

To a mixture of HL (1 mmol) and KOH (1 mmol) in 50 ml of water, $ZnCl_2$ (1 mmol) was added under stirring, resulting a pH 6.5 solution. After 24 h at room temperature (r.t.) an orange crystalline solid appeared, which being submerged in the mother liquor keeps both its crystalline appearance and stoichiometry; otherwise, if it is filtered off, washed with ethanol and ether, and dried over P_4O_{10} results in a powdered solid phase of $[ZnL_2(H_2O)_4]$ stoichiometry. *Anal.* Calc. for $ZnC_{14}H_{24}N_{10}O_{12}$: C, 28.51; H, 4.07; N, 23.75. Found: C, 28.36; H, 4.26; N, 23.62%. Thermal data: Dehydration processes $[ZnL_2(H_2O)_4]\rightarrow[ZnL_2]$ occur in the 50–240°C temperature range, corresponding to a weight loss of 12.10% (calc. for $4H_2O$: 12.22%). In the DSC appear as four endothermic effects centred at 93.3, 144.8, 168.8 and 206.3°C with ΔH of -46.31, -7.66, -16.50 and -14.32 kJ mol^{-1}, respectively. Pyrolysis of ZnL_2 starts at 250°C and ends at 760°C to yield ZnO as residue (13.8%).

2.2.2. $\{[Cd(\mu\text{-}L)Cl(H_2O)_2]\cdot H_2O\}_n$ (**2**)

To a mixture of HL (1 mmol) and KOH (1 mmol) in 50 ml of water, $CdCl_2$ (1 mmol) was added, resulting a pH 6.0 solution. This was evaporated at r.t. appearing a rose solid which was filtered off and despised. Five days later a violet crystalline solid appeared, which was collected, washed with ethanol and ether, and dried over P_4O_{10}. *Anal.* Calc. for $CdC_7H_{14}N_5O_7Cl$: C, 19.63; H, 3.27; N, 16.36. Found: C, 19.65; H, 3.03; N, 16.10%. Thermal data: Dehydration process $\{[Cd(\mu\text{-}L)Cl(H_2O)_2]\cdot H_2O\}_n\rightarrow[CdLCl]$ occurs in the temperature range 60–180°C, appearing as two overlapped endothermic effects in the DSC curve with an averaged

Table 1
Crystal data and structure refinement for **1** and **2**

Complex	**1**	**2**
Empirical formula	$ZnC_{14}H_{36}N_{10}O_{18}$	$C_7H_{14}N_5O_7ClCd$
Formula weight	697.90	428.08
Temperature (K)	293(2)	293(3)
Wavelength (Å)	0.71069	0.71073
Crystal system	triclinic	triclinic
Space group	$P\bar{1}$	$P\bar{1}$
Unit cell dimensions		
a (Å)	7.453(2)	6.7316(11)
b (Å)	8.290(2)	9.4810(14)
c (Å)	12.724(3)	11.087(2)
α (°)	105.835(5)	83.695(8)
β (°)	91.058(5)	77.616(8)
γ (°)	109.73(5)	77.190(8)
Z	1	2
V (Å^3)	706.6(3)	672.5(2)
D_{calc} (g cm^{-3})	1.640	2.114
Absorption coefficient (mm^{-1})	0.966	1.866
$F(000)$	364	424
Crystal size (mm)	$0.25\times0.20\times0.35$	$0.30\times0.20\times0.08$
θ range (°)	$1.68\leq\theta\leq29.99$	$1.80\leq\theta\leq30.0$
Limiting indices	$-10\leq h\leq10$ $-11\leq k\leq11$ $0\leq l\leq17$	$-1\leq h\leq8$ $-13\leq k\leq13$ $-15\leq l\leq15$
Reflections collected	8234	4630
Independent reflections	4117 [$R_{int}=0.0018$]	3706 [$R_{int}=0.0186$]
Refinement method	full-matrix least-squares on F^2	full-matrix least-squares on F^2
Data/restraints/ parameters	4109/0/196	3706/0/190
Goodness-of-fit (F^2)	1.090	1.043
R indices [$I>2\sigma(I)$]	$R_1=0.0494$ $Rw_2=0.1282$	$R_1=0.0231$ $Rw_2=0.0601$
Largest peak and hole (e Å^{-3})	0.636 and -0.714	0.535 and -0.535

ΔH of -51.0 kJ mol^{-1}, corresponding to a weight loss of 12.26% (calc. for $3H_2O$: 12.61%). Pyrolysis of [CdLCl] occurs in the temperature range of 220–800°C to yield CdO (18.53%) and sublimated $CdCl_2$.

2.3. X-ray data collection and structure determination

Single-crystal data collection for **1** were obtained from a crystal submerged in the mother liquors in a Lindeman capillary tube. Data collection for **1** and **2** were performed at 293 K with a Siemens R 3m/V diffractometer using graphite monochromatized using graphite Mo Kα radiation. Crystal data and details of the structure determination are included in Table 1. The unit cell parameters were calculated by least-squares refinement of 25 well centred reflections in the range $15<2\theta<45°$. The data were collected by $\omega/2\theta$ scan mode and were corrected for Lorenz and polarisation effects. Absorption correction were applied via an empirical ψ-scan. Structures were solved by direct methods and subsequent Fourier syntheses with the SHELXTL-PC V5.0 package [15]. Non-hydrogen atoms were refined anisotropically in the final cycles, while hydrogen were placed at their calculated position and were refined isotropically riding on the previous atoms. Neutral atomic scattering and dispersion factors were those included in the SHELXTL-PC program.

3. Results and discussion

3.1. Solution study

The acid–base behaviour of this family of N-pyrimidine aminoacids (see Scheme 1) is, as could be expected, qualitatively similar. The first protonation process involves the carboxylate group whereas the second protonation occurs on the pyrimidine ring [7]. Nevertheless, the pH values at which these processes take place significantly vary within this series of compounds, as shown in Table 2, which is due to the different nature of the R group on the aminoacid rest. In view of this, we are investigating the coordinative behaviour of these ligands toward different metal ions, such as Zn(II) and Cd(II), in aqueous medium.

The potentiometric study of the 1:1 [M(II)]/[HL] systems (where HL stands for N-2-(4-amino-1,6-dihydro-1-methyl-5-nitroso-6-oxopyrimidinyl)glycine and M(II) = Zn and Cd) points out a rather weak interaction between the ligand and the metal ions, where only the $M(OH)_2$ species were detected [9], which could be indicative of dissociation processes of the possible adducts formed.

The best fit of the experimental results obtained from solutions with 1:4 [Zn(II)]/[HL] ratio corresponds to the equilibria given in Table 2 ($\sigma_{fit}=0.0071$). Although the $Zn(HL)^{2+}$ species exists in little extension (Fig. 1) it was included in the postulated model because it af-

Table 2
Solution data

Species (pqr)	Process	Log β	Reference
(011)	$L^-+H^+=HL$	3.98(3)	[10]
(011)	$(L^1)^-+H^+=HL^1$	3.34(1)	[7]
(011)	$(L^2)^-+H^+=HL^2$	3.88(3)	[8]
(012)	$L^-+2H^+=H_2L^+$	6.54(4)	[10]
(012)	$(L^1)^-+2H^+=(H_2L^1)^+$	4.89(3)	[7]
(012)	$(L^2)^-+2H^+=(H_2L^2)^+$	6.30(4)	[8]
(111)	$Zn^{2+}+L^-+H^+=Zn(HL)^{2+}$	5.28(4)	this work
(120)	$Zn^{2+}+2L^-=Zn(L)_2$	7.61(2)	this work
(111)	$Cd^{2+}+L^-+H^+=Cd(HL)^{2+}$	5.44(9)	[9]
(120)	$Cd^{2+}+2L^-=Cd(L)_2$	7.47(9)	[9]
($10\bar{2}$)	$Zn^{2+}=Zn(OH)_2+4H^+$	$-15.56(1)$	this work
($10\bar{4}$)	$Zn^{2+}=Zn(OH)_4^{2-}+4H^+$	$-30.20(3)$	this work

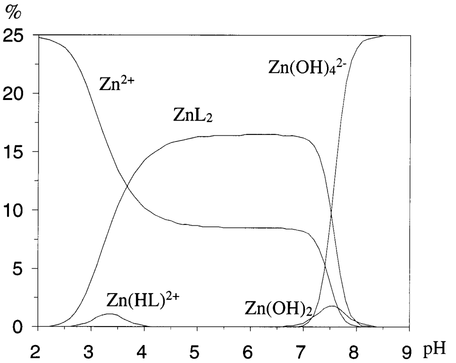

Fig. 1. Distribution species diagram for [Zn(II)]/[HL] at 1:4 molar ratio versus pH.

forded an improvement in the σ_{fit} value. At 1:4 metal-to-ligand ratio both metal ions, Zn(II) and Cd(II) [9], exhibit a similar behaviour. Thus, very close log β values are obtained for the $M(HL)^{2+}$ and ML_2 species (Table 2), being lower to those observed for the Cu(II)/HL system [10]. For the $M(HL)^{2+}$ complexes the carboxylate group remains protonated, by which the coordination likely takes place through the exocyclic nitroso and oxo groups of the pyrimidine ring, at it has been observed for the related 4-amino-5-nitroso-6-oxopyrimidine base [16]. As for the ML_2 species the log β_{120} values are still lower than that of CuL_2 but less than for the former $M(HL)^{2+}$ complexes, which is indicative that when the carboxylate group is the primary coordination site the reactivity of the ligand increases [7–9]. Nevertheless, it has to be pointed out the different behaviour exhibited by the HL ligand with Zn(II) and Cd(II) compared to the related HL^1 (see Scheme 1). Thus, in the case of the HL^1 only the ZnL^1_2 [log $\beta = 6.42(1)$] and $Cd(HL)^{2+}$ [log $\beta = 6.81(8)$] species were detected [7]. In order to elucidate the effect of the R substituent on the aminoacid moiety we are working with the related alanine- and valine- derivatives, HL^2 and HL^3, respectively (Scheme 1).

3.2. Solid study

Complexes $[Zn(L)_2(H_2O)_4]{\cdot}6H_2O$ (**1**) and $\{[Cd(\mu\text{-}L)Cl(H_2O)_2]{\cdot}H_2O\}_n$ (**2**) were obtained by reacting the corresponding metal(II) chloride with the deprotonated L ligand in a 1:1 ratio. When the *N*-pyrimidine aminoacids ligands act deprotonated their primary coordination site is the carboxylate group. In addition to this, these ligands are able to use the pyrimidine moiety, which is the primary coordination site when they act in neutral form, to yield polynuclear complexes. This fact is also favoured by a 1:1 metal-to-ligand ratio since the metal can complete its coordination sphere by interacting with additional ligands, which act bridging two or more metal ions [7,8,10].

In this line, the related Zn(II) and Cd(II) complexes obtained by us with the methionine derivative (HL^1) show a supramolecular 2D layered structure in which the R groups ($R = CH_2CH_2SCH_3$), see Scheme 1, are oriented to the external surfaces of the layers, resulting in an interlayer separation of approximately 11 Å [7]. Therefore, one might expect that by replacing the HL^1

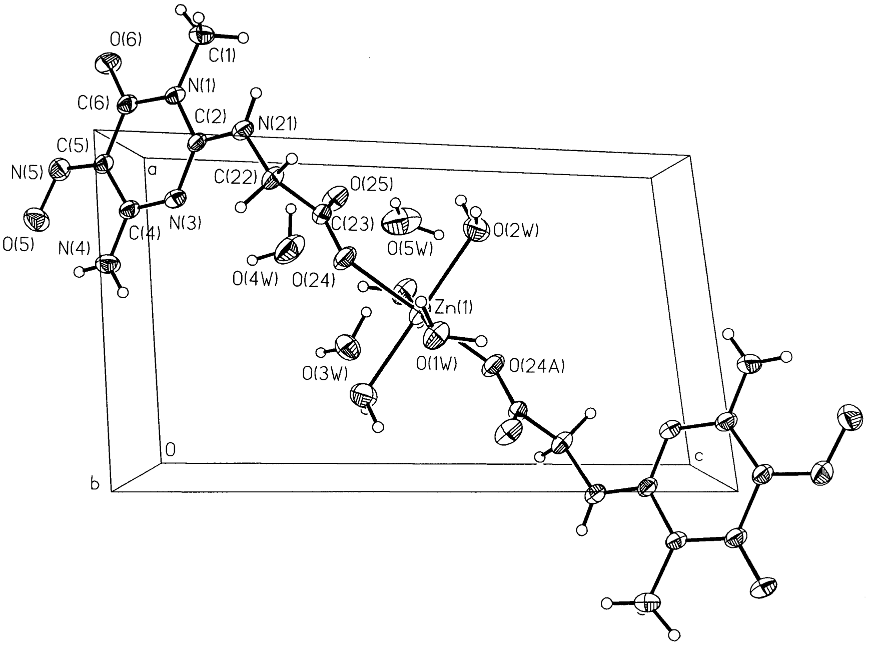

Fig. 2. A perspective view of complex **1** (ellipsoids represent 40% of probability).

Table 3
Selected bond lengths (Å) and angles (°) [a]

Complex **1**			
Zn(1)–O(24)	2.083(2)	Zn(1)–O(24)^{I}	2.083(2)
Zn(1)–O(1w)	2.053(2)	Zn(1)–O(1w)^{I}	2.053(2)
Zn(1)–O(2w)	2.196(2)	Zn(1)–O(2w)^{I}	2.196(2)
O(1w)–Zn(1)–O(1w)^{I}	180.0	O(24)^{I}–Zn(1)–O(2w)	92.60(9)
O(1w)^{I}–Zn(1)–O(24)^{I}	90.04(7)	O(24)–Zn(1)–O(2w)	87.40(9)
O(1w)–Zn(1)–O(24)^{I}	89.96(7)	O(1w)^{I}–Zn(1)–O(2w)^{I}	91.53(9)
O(1w)^{I}–Zn(1)–O(24)	89.96(7)	O(1w)–Zn(1)–O(2w)^{I}	88.47(9)
O(1w)–Zn(1)–O(24)	90.04(7)	O(24)^{I}–Zn(1)–O(2w)^{I}	87.40(9)
O(24)^{I}–Zn(1)–O(24)	180.0	O(24)–Zn(1)–O(2w)^{I}	92.60(9)
O(1w)^{I}–Zn(1)–O(2w)	88.47(9)	O(2w)–Zn(1)–O(2w)^{I}	180.0
O(1w)–Zn(1)–O(2w)	91.53(9)		
Complex **2**			
Cd(1)–O(1W)	2.350(2)	Cd(1)–N(5)	2.455(2)
Cd(1)–O(24)	2.361(2)	Cd(1)–O(23)	2.469(2)
Cd(1)–O(2W)	2.361(2)	Cd(1)–Cl(1)	2.5667(7)
Cd(1)–O(6)	2.3834(14)	O(1w)–Cd(1)–O(24)	134.56(6)
O(1w)–Cd(1)–O(2w)	86.54(7)	O(24)–Cd(1)–O(2W)	89.80(6)
O(1W)–Cd(1)–O(6)	76.34(6)	O(24)–Cd(1)–O(6)	148.24(5)
O(2W)–Cd(1)–O(6)	84.54(6)	O(1W)–Cd(1)–N(5)	144.01(6)
O(24)–Cd(1)–N(5)	80.47(5)	O(2W)–Cd(1)–N(5)	85.70(6)
O(6)–Cd(1)–N(5)	67.96(5)	O(1W)–Cd(1)–O(23)	80.47(6)
O(24)–Cd(1)–O(23)	54.32(5)	O(2W)–Cd(1)–O(23)	90.96(7)
O(6)–Cd(1)–O(23)	156.60(5)	N(5)–Cd(1)–O(23)	134.71(5)
O(1W)–Cd(1)–Cl(1)	91.21(5)	O(24)–Cd(1)–Cl(1)	95.80(5)
O(2W)–Cd(1)–Cl(1)	173.90(5)	O(6)–Cd(1)–Cl(1)	89.42(4)
N(5)–Cd(1)–Cl(1)	92.85(4)	O(23)–Cd(1)–Cl(1)	94.26(5)

[a] $I = -x+1,\ -y+1,\ -z+1$.

ligand by HL, where R = H, and working in identical conditions we would obtain bidimensional polynuclear complexes with reduced interlayer separation. Despite of this, complex **1** consists of neutral mononuclear entities in which the zinc ion is hexacoordinated by two L ligands, completing the coordination sphere with four water molecules, as depicted in Fig. 2. Selected bond lengths and angles are listed in Table 3. The six ligands are arranged around the Zn(II) ion in a distorted octahedral geometry, with the metal ion lying on a C_i centre. In this description two water molecules and two monodentate carboxylate groups forms the equatorial plane while the two remaining water molecules occupy the axial positions at a longer distance (see Table 3). The coordination mode of the ligand is also evident from the IR spectrum; where the $\nu(CO_2^-)_{symm.}$ band in the uncoordinated ligand is shifted to lower frequency while the ν(C=O) and ν(N=O) bands remain practically unaffected (Table 4). In addition to this, the NMR data also support this coordination mode, since the ^{13}C-signal belonging to the COO$^-$ group is shifted to lower field with respect to the L ligand, whereas the C_{α}, C(5) and C(6) signals remain practically unaffected, see Table 4. Remaining bond lengths and angles are similar to those reported for similar structures [17–20], and do not deserve additional comments. The tridimensional structure of **1** is achieved by an extended and complicated hydrogen bonding network involving the coordinated and the six lattice water molecules and the L ligands. These lattice water molecules are lost very easily, by which the crystal structure was solved submerging the crystal in the mother liquor. Within this network of hydrogen bonding it is noteworthy to mention the intramolecular hydrogen bond between the N(4)H$_2$ and the O(5) atom, which is retained in dmso solutions as reveal the ^{1}H NMR signals listed in Table 4. This hydrogen bond has only not been observed when the pyrimidine moiety coordinates in a chelating fashion through the O(5)/O(6) atoms [16].

On the other hand, complex **2** consists of infinite chains running approximately perpendicular to the *ab* plane, see Fig. 3. Within the polynuclear structure each Cd(II) is heptacoordinated by two bidentate L ligands, two water molecules and a Cl$^-$ ion, being the mononuclear fragment: Cd(μ-L)Cl(H$_2$O)$_2$. This heptacoordination for a cadmium(II) ion, which can be described as a distorted pentagonal bipyramid with the O(2w) and Cl(1) occupying the axial positions, is not unusual and have been found for complexes with related ligands [21–23]. The coordination mode of the ligand can by described as a bis-didentate-bridging mode, linking the metal ions through the pyrimidine and the carboxylate group to yield a metal-metal intrachain distance of 11.671 Å. The IR spectrum is, as expected, consistent with this coordination mode. Thus, in **2** the ν(NO) and ν(CO) bands are also shifted to lower frequencies, as well as the $\nu(CO_2^-)_{symm}$ band (Table 4). The NMR data are, as in **1**, also consistent with a coordination of the ligand to the Cd(II) ion only through the carboxylate group, as reveals the displacement to lower field of the COO$^-$ signal and the unaffected displacements of

Table 4
Selected IR, ^{1}H and ^{13}C NMR data

	KL·H$_2$O	**1**	**2**
ν(OH) + ν(NH) [a]	3458, 3239	3470, 3353, 3229	3426, 3357
ν(C(6)=O)	1688	1691	1657
$\nu(CO_2)_{symm}$	1622	1602	1598
ν(NO)	1495	1497	1455
δ N(4)H$_2$ [b]	10.93, 8.34	10.90, 8.30	10.83, 8.35
δ C(α)H$_2$	3.59	3.96	4.03
δ C(α) [c]	46.12	45.01	44.02
δ CO$_2$	168.68	172.78	174.16
δ C(6)=O	168.61	161.66	161.68
δ C(5)–NO	141.92	141.11	141.42

[a] IR: cm^{-1} (KBr).
[b] ^{1}H NMR: δ(ppm), dmso-d$_6$.
[c] ^{13}C NMR: δ(ppm), dmso-d$_6$.

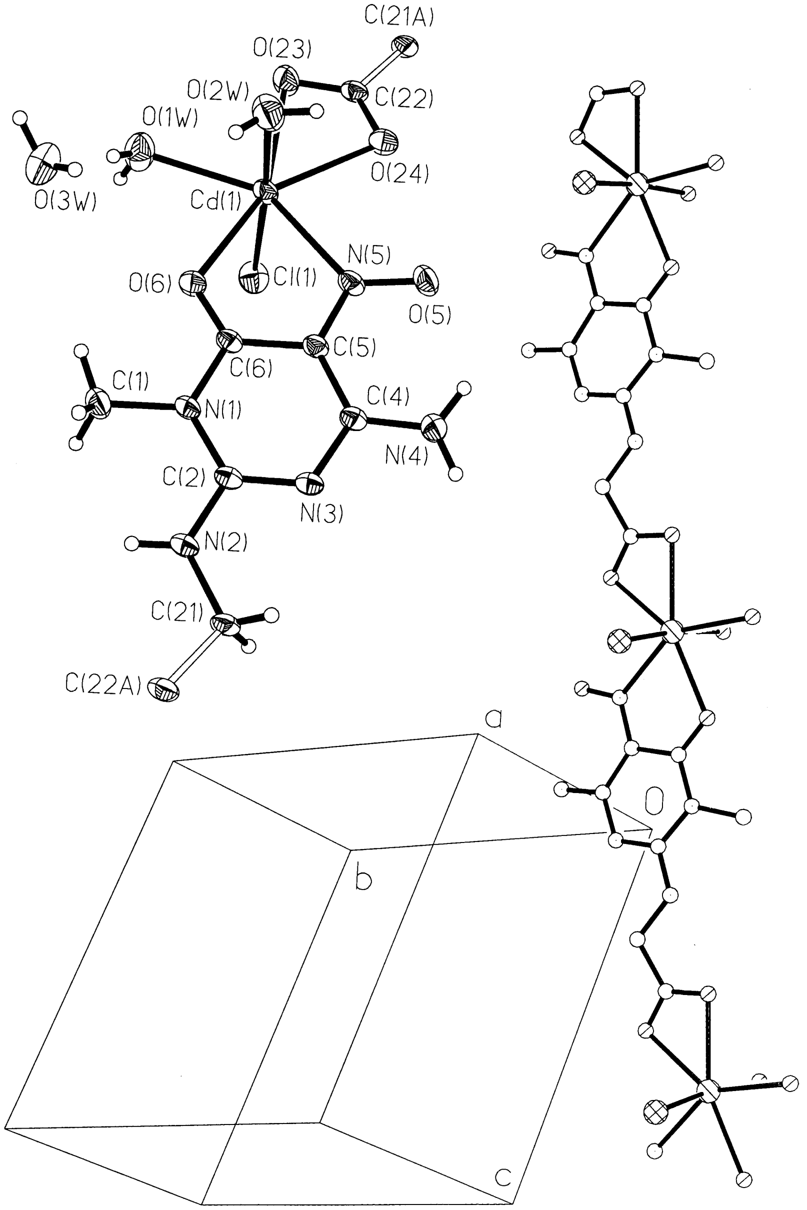

Fig. 3. Perspective views of the mononuclear fragment and a chain of complex **2** (ellipsoids represent 40% of probability).

the C_α, C(5) and C(6) signals, see Table 4. Obviously, this fact indicates that the polynuclear structure is not retained in dmso solutions, being the pyrimidine–metal bond the cleavage point, which, in turn, is in agreement with the aqueous solution results since the primary coordination site when the ligand acts deprotonated is the carboxylate group.

Bond distances and angles are usual for Cd(II) complexes, except for N(5) and O(23) which are slightly longer due to the steric crowding present in both chelate rings [21–24].

Finally, it has to be noted again, the important effect of the R-substituent in the reactivity of this family of ligands. The different reactivity is not only evident from the solution studies but also from the corresponding metal complexes isolated in solid state. Thus, the HL ligand shows a marked trend to form complexes of lower dimensionality when compared to HL^1, since for Zn(II) a mononuclear complex has been obtained while for Cd(II), although the complex is polynuclear, is monodimensional and not bidimensional as in the case of HL^1. Nevertheless, more examples of this family of ligands are needed in order to understand all the factors, and in particular the role of the substituent R on the C_α, in which we are currently working.

Acknowledgements

The authors thank Junta de Andalucía for financial support.

References

[1] B. Kaitner, N. Paulic, N. Raos, J. Coord. Chem. 25 (1992) 95.
[2] N. Paulic, N. Raos, J. Coord. Chem. 31 (1994) 181.
[3] N. Raos, J. Mol. Struct. 355 (1995) 211.
[4] J. Sabolovic, K. Rasmussen, Inorg. Chem. 34 (1995) 1221.
[5] D.B. Grotjahn, C. Joubran, Organometallics 15 (1996) 1230.
[6] M.A. Díaz-Díez, F.J. García-Barros, C. Valenzuela-Calahorro, J. Inorg. Biochem. 56 (1994) 243.
[7] R. Lopez-Garzon, P. Arranz-Mascarós, M.L. Godino-Salido, M.D. Gutierrez-Valero, J.M. Moreno, Inorg. Chim. Acta, (1999) in press.
[8] P. Arranz-Mascarós, M.L. Godino-Salido, R. López-Garzón, M.D. Gutiérrez-Valero, J.M. Moreno, Polyhedron 18 (1999) 793.
[9] P. Arranz-Mascarós, R. López-Garzón, M.L. Godino-Salido, M.D. Gutiérrez-Valero, Transit. Met. Chem. 23 (1998) 501.
[10] J.M. Moreno, P. Arranz-Mascarós, R. López-Garzón, M.D. Gutiérrez-Valero, M.L. Godino-Salido, J. Cobo-Domingo, Polyhedron 18 (1999) 1635.
[11] M.L. Godino-Salido, M.D. Gutierrez-Valero, R. López-Garzón, J.M. Moreno, Inorg. Chim. Acta 221 (1994) 127.
[12] G. Gran, Analyst 77 (1952) 661.
[13] A. Liberti, T.S. Light, J. Chem. Ed. 39 (1962) 236.
[14] A.E. Martell, R.J. Motekaitis, The Determination and Use of Stability Constants, VCH, New York, 1992.
[15] SHELXTL-PC V5.0, Siemens Analytical X-ray Instruments, Madison, WI, 1995.
[16] P. Arranz-Mascarós, M.L. Godino-Salido, R. López-Garzón, M.D. Gutiérrez-Valero, J.M. Moreno, Polyhedron 18 (1999) 689.
[17] H. Grewe, M.R. Udupa, B. Krebs, Inorg. Chim. Acta 63 (1982) 119.
[18] A. Fuertes, C. Miravitlles, E. Escriva, E. Coronado, D. Beltran, L. Padel, J. Chem. Soc., Dalton Trans. (1989) 863.
[19] X-M. Chen, X-C. Huang, M-L Tong, Y-X. Tong, S.W. Ng, Aus. J. Chem. 50 (1997) 865.
[20] N. Lalioti, C.P. Rastopoulou, A. Terzis, A. Panagiotopoulos, S.P. Perlepes, E. Manessi-Zoupa, J. Chem. Soc., Dalton Trans. (1998) 1327.
[21] N. Nakasuka, S. Azuma, M. Tanaka, Acta Crystallogr., Sect. C 42 (1986) 1736.
[22] H.C. Lopez-Sandoval, N. Barba-Behrens, S. Bernes, N. Farfan-Garcia, H. Hopfl, J. Chem. Soc., Dalton Trans. (1997) 3415.
[23] E. Bermejo, A. Castiñeiras, R. Domínguez, J. Strähle, C. Maichle-Mössmer, Polyhedron 15 (1996) 1923 and refs. therein; K.H. Chung, E. Hong, Y. Do, C.H. Moon, J. Chem. Soc., Dalton Trans. (1996) 3363 and refs. therein.
[24] C.I.H. Ashby, W.F. Paton, T.L. Brown, J. Am. Chem. Soc. 102 (1980) 2990.